

See discussions, stats, and author profiles for this publication at: <https://www.researchgate.net/publication/7478388>

# Structure–activity relationship study of homoallylamines and related derivatives acting as antifungal agents

ARTICLE *in* BIOORGANIC & MEDICINAL CHEMISTRY · APRIL 2006

Impact Factor: 2.79 · DOI: 10.1016/j.bmc.2005.10.036 · Source: PubMed

CITATIONS

32

READS

41

## 7 AUTHORS, INCLUDING:



**Fernando D Suvire**

Universidad Nacional de San Luis

44 PUBLICATIONS 396 CITATIONS

SEE PROFILE



**Vladimir V. Kouznetsov**

Industrial University of Santander

226 PUBLICATIONS 1,849 CITATIONS

SEE PROFILE



**Susana Zacchino**

Rosario National University

162 PUBLICATIONS 2,494 CITATIONS

SEE PROFILE



**Ricardo Daniel Enriz**

Universidad Nacional de San Luis

131 PUBLICATIONS 1,909 CITATIONS

SEE PROFILE

## Structure–activity relationship study of homoallylamines and related derivatives acting as antifungal agents

Fernando D. Suvire,<sup>a</sup> Maximiliano Sortino,<sup>c</sup> Vladimir V. Kouznetsov,<sup>b</sup>  
Leonor Y. Vargas M.,<sup>b</sup> Susana A. Zacchino,<sup>c</sup> Uriel Mora Cruz<sup>b</sup> and Ricardo D. Enriz<sup>a,\*</sup>

<sup>a</sup>*Facultad de Química, Bioquímica y Farmacia, Universidad Nacional de San Luis (U.N.S.L.),  
Chacabuco 917, 5700 San Luis, Argentina*

<sup>b</sup>*Laboratorio de Química Orgánica y Biomolecular, Escuela de Química, Universidad Industrial de Santander,  
A.A. 678 Bucaramanga, Colombia*

<sup>c</sup>*Farmacognosia, Facultad de Ciencias Bioquímicas y Farmacéuticas, Universidad Nacional de Rosario,  
Suipacha 531, 2000 Rosario, Argentina*

Received 9 September 2005; revised 19 October 2005; accepted 20 October 2005  
Available online 10 November 2005

**Abstract**—The synthesis, in vitro evaluation, and structure–activity relationship studies of homoallylamines and related derivatives acting as antifungal agents are reported. Among them, compounds *N*-(4-bromophenyl)-*N*-(2-furylmethyl)amine and *N*-(4-chlorophenyl)-*N*-(2-furylmethyl)amine reported here exhibited remarkable antifungal activity against dermatophytes. Theoretical calculations allow us to determine the minimal structural requirements to produce the antifungal response and can provide a guide for the design of compounds with these properties.

© 2005 Elsevier Ltd. All rights reserved.

### 1. Introduction

The current interest in the development of new antifungal agents can partially be due to the dramatic rise in the number of AIDS cases and the subsequent suppression of the immune system in patients with the disease. Other conditions that have spurred the development of new antifungal agents include the increase in the frequency of bone marrow and organ transplants, the use of antineoplastic agents, long-term use of corticoids, and even the indiscriminate use of antibiotics.<sup>1–3</sup> On the other hand, the emergence of fungal resistance to currently available antifungal agents, specially azoles, leads to an increasing need for new and effective antifungal agents.<sup>4</sup>

Owing to their eukaryotic nature, fungal cells have only a restricted set of specific targets that do not overlap with their mammalian counterparts.<sup>5</sup> The cell wall of most fungi offers a selective target for drug design because several enzymes involved in the synthesis of specific components of the fungal cell wall are not found in human cells.<sup>5,6</sup> The fungal cell wall consists of a rigid

shell that surrounds and protects the cell against environment and mechanical stress.<sup>7</sup> With considerable variation among different species, the main components of cell wall of most fungi include chitin,  $\beta$ - or  $\alpha$ -linked glucans, and a variety of mannoproteins.<sup>8</sup>

In the course of our ongoing screening program for new and selective antifungal compounds, we have previously reported the antifungal activity of different compounds obtained from natural<sup>9–12</sup> and synthetic<sup>13–18</sup> sources. Among them, a series of 4-aryl- or 4-alkyl-*N*-arylamino-1-butenes ('homoallylamines') and related tetrahydroquinolines and quinolines<sup>16</sup> display a range of antifungal properties against dermatophytes, which are responsible for most dermatomycoses in humans. More recently, we extended our study introducing a new series of 4-*N*-arylamino-1-butenes containing the pyridinyl or quinolinyl moieties at C4 and other structurally related compounds.<sup>17</sup> Regarding their mode of action, active compounds showed in vitro inhibitory activities against (1,3) $\beta$ -D-glucan-synthase and mainly against chitin-synthase, enzymes that catalyze the synthesis of major fungal cell wall polymers.<sup>7,8</sup> Since fungal but not mammalian cells possess a cell wall, these structures appeared as promising leads for the development of selective antifungal compounds.

**Keywords:** Homoallylamines; Antifungal activity; SAR; Synthesis.

\* Corresponding author. E-mail: [denriz@unsl.edu.ar](mailto:denriz@unsl.edu.ar)

In an attempt to improve the biological profile of homoallylamines, we present here the synthesis and antifungal activity of 15 additional heterocyclic analogues not reported previously with or without the allylamine group.

With both, the results reported here, and the previously published data,<sup>16,17</sup> we have performed a comprehensive structure–activity relationship (SAR) study on 43 molecules (20 homoallylamines and 23 structural analogues), in order to determine the minimal structural requirements for these compounds to produce the antifungal effect.

We also discuss a possible pharmacophore model for these compounds and the stereoelectronic requirements necessary to elicit the activity.

## 2. Results and discussion

### 2.1. Chemistry

The *N*-arylaldehydes, principal starting materials in this investigation, were prepared from commercially available aromatic aldehydes (benzaldehydes, 2-furaldehydes, and 2-thiophenecarboxyaldehyde) and substituted anilines according to literature procedures.<sup>16,19</sup> New series of obtained aldimines were converted into secondary *N*-benzylanilines **12–14** (structure I in Table 1), *N*-(2-furylmethyl)anilines **34–40**, *N*-(2-thienylmethyl)anilines **41–43** (Table 2) or *N*-aryl-*N*-[1-(thien-2-yl)but-3-enyl]amines **44**, **45** ('homoallylamines'<sup>20</sup>) (structure III). Because the reduction of aldimines with an excess of NaBH<sub>4</sub> in the methanol is still the reaction of choice to produce secondary amines in a reasonably good yield, we employed this method in our work. Thus, first series was easily prepared obtaining these secondary amines as a colored solid or liquid in 75–98% yields after purification using a SiO<sub>2</sub> chromatography column. Using the nucleophilic addition of allylmagnesium bromide to the C=N bond of respective aldimines, we prepared new homoallylamines, which were isolated as stable oils in 70–77% yields (Scheme 1). *N*-Substituted anilines **12–14**, **34–40**, and **41–43** were synthesized according to reported methodologies.<sup>21,22</sup>

Compounds **1** and **2** were easily prepared from the respective aldimines using the Grignard reaction with allylmagnesium bromide. Compound **22** was obtained from compound **1** under acidic intramolecular cyclization.<sup>16,17</sup>

### 2.2. Structure–antifungal activity relationship study

Our previous works<sup>16,17</sup> provided a considerable diversity of chemical structures of antifungal homoallylamines and their derivatives, most compounds possessing two aromatic rings with a flexible or a rigid connecting unit.

With the aim of understanding the experimental results, we grouped these compounds into three main classes, according to the type of connection between both aromatic rings:

- (a) Compounds containing a flexible connecting chain (homoallylamines).
- (b) Compounds containing a conformationally restricted non-aromatic connecting ring (tetrahydroquinolines).
- (c) Compounds containing a conformationally restricted aromatic connecting ring (quinolines).

How can theoretical calculations contribute to the understanding of the activity of these molecules? One way is to study a series of chemically related compounds and to obtain more precise information about how the different members of a series resemble each other in terms of spatial orientations for the recognition of the receptor. These differences may be correlated with the antifungal activities.

We conducted a computer-assisted conformational and electronic study on the most representative molecules of each series.

Regarding conformational analysis RHF/6-31G(d) calculations on compounds **3** and **15** were carried out and the low-energy conformations obtained for these homoallylamines were compared with those previously reported for tetrahydroquinolines and quinolines.<sup>18</sup> Tetrahydroquinoline molecules were shown to possess eight distinct forms (without considering enantiomeric forms), varying in the orientation of both substituents, CH<sub>3</sub> group and pyridinyl ring.<sup>18</sup> The preferred conformation adopted by homoallylamines is closely related to those previously reported for tetrahydroquinolines<sup>18</sup> (Fig. 1). In contrast, quinoline derivatives display a quasi-planar conformation as the preferred form, which is not viable for tetrahydroquinoline (and homoallylamines) structures due to the sp<sup>3</sup> form of their chiral carbon.

Taking into account this difference, we here focused this study on tetrahydroquinolines and homoallylamines. Quinoline derivative SAR studies will be reported in a separate paper.

The antifungal activities obtained for homoallylamines and tetrahydroquinolines are summarized in Tables 1 and 2.

To evaluate the SARs, the effects of structural changes in three regions of the molecules were considered: variation in the A and B rings as well as in the connecting chain (see a general structure in Scheme 2).

**2.2.1. Role of ring B.** We have previously reported that the change of the phenyl ring B by heterocyclic rings such as  $\alpha$ -,  $\beta$ - or  $\gamma$ -pyridine (compounds **15–21**, **23–31** in Table 1) gives very active compounds. In the present paper, we extend the range of heterocyclic rings replacing phenyl ring by other heterocycles such as furan (compounds **34–40**) and thiophene (**41–45**). Interesting enough, some of them displayed remarkable activity (compounds **38**, **39**, **41–43**, and **45** MIC = 3.25–50  $\mu$ g/ml) (Table 2), giving further support for the bio-isosteric nature of these alternative aromatic rings.

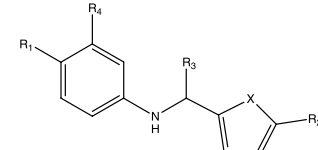
**Table 1.** MIC values ( $\mu\text{g/ml}$ ) of homoallylamines and related compounds acting against dermatophytes

|--|--|--|--|--|--|--|--|--|--|--|--|--|--|--|

Mc, *Microsporum canis* C 112; Mg, *Microsporum gypseum* C 115; Tr, *Trichophyton rubrum* C 110; Tm, *Trichophyton mentagrophytes* ATCC 9972; Ef, *Epidermophyton floccosum* C 114. Amp., Amphotericin B; Ket., Ketoconazole; Terb., Terbinafine.

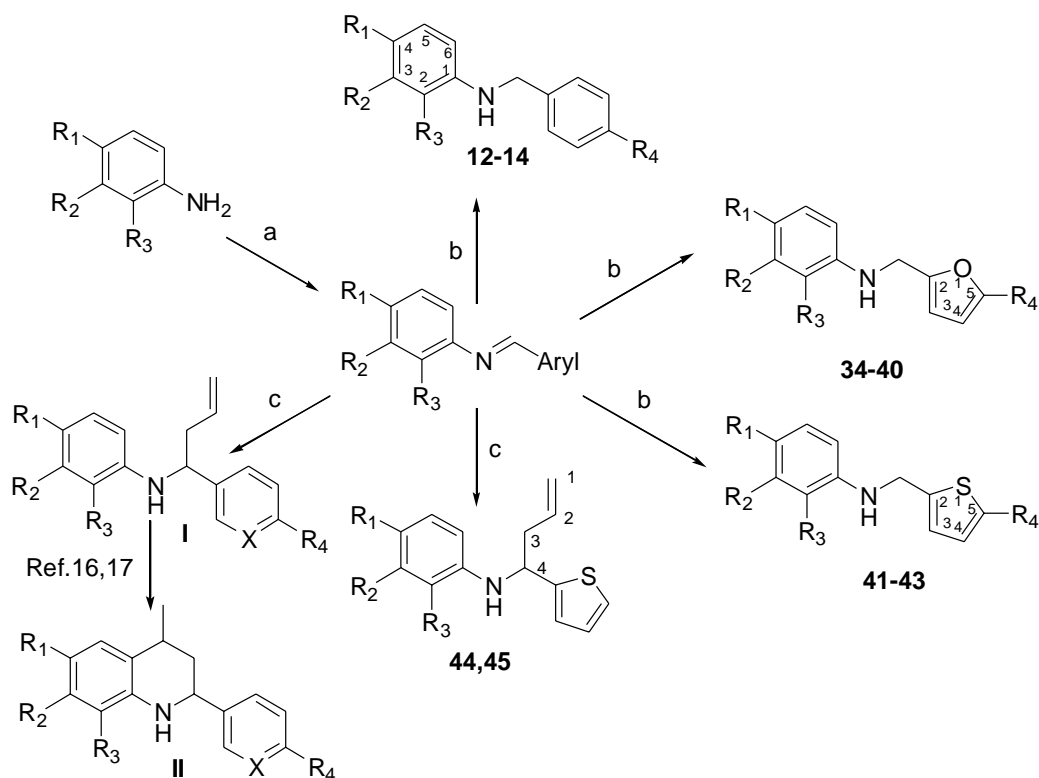
From the calculated electron distribution in the molecule, some properties such as the net atomic charges and bond polarities can be predicted, which help us to characterize the nature of interactions at specific receptor sites. The electron distribution can also be used to quantitatively map the electrostatic potential generated by a molecule in all regions surrounding it.<sup>23</sup>

The molecular electrostatic potentials (MEPs) for compounds **7** and **15** (Fig. 2) show a closely related stereo-electronic behavior for both compounds. The 0.002 el/au<sup>3</sup> MEP maps of molecules **7** and **15** show three clear minima  $V_{(r)\min}$ , being the lowest-energy minima the zone located in the in-plane lone pair region of N in compound **15**, and the minimum located in the proximity

**Table 2.** MIC values ( $\mu\text{g/ml}$ ) of related compounds acting against dermatophytes


ID	Substituents					Activity				
	R <sub>1</sub>	R <sub>2</sub>	R <sub>3</sub>	R <sub>4</sub>	X	Mc	Mg	Tm	Tr	Ef
34	H	H	H	H	O	>50	>50	>50	>50	>50
35	H	CH <sub>3</sub>	H	H	O	50	50	25	50	50
36	OCH <sub>3</sub>	H	H	H	O	>50	>50	50	>50	50
37	OCH <sub>3</sub>	CH <sub>3</sub>	H	H	O	>50	50	50	25	50
38	Br	H	H	H	O	6.25	6.25	12.5	3.125	3.125
39	Cl	H	H	H	O	12.5	12.5	12.5	6.25	12.5
40	F	H	H	H	O	62.5	>50	>50	25	25
41	H	H	H	H	S	25	25	25	12.5	12.5
42	H	H	H	CH <sub>3</sub>	S	12.5	12.5	25	12.5	12.5
43	CH <sub>3</sub>	H	H	H	S	25	12.5	50	25	12.5
44	H	H	Allyl	H	S	125	125	125	125	125
45	CH <sub>3</sub>	H	Allyl	H	S	6.25	50	6.25	12.5	6.25
Ket.						15	6.25	6.25	6.25	25
Amp.						50	12.5	12.5	12.5	0.3
Terb.						0.01	0.006	0.006	0.003	0.004

Mc, *Microsporum canis* C 112; Mg, *Microsporum gypseum* C 115; Tr, *Trichophyton rubrum* C 110; Tm, *Trichophyton mentagrophytes* ATCC 9972; Ef, *Epidermophyton floccosum* C 114. Amp., Amphotericin B; Ket., Ketoconazole; Terb., Terbinafine.



**Scheme 1.** Preparation of N-substituted anilines and homoallylamines. Reagents and conditions: (a) ArCHO, EtOH (benzene or toluene), rt to reflux; (b) NaBH<sub>4</sub>, MeOH, rt to reflux; (c) allylmagnesium bromide/Et<sub>2</sub>O, 15–34 °C, then H<sub>2</sub>O/NH<sub>4</sub>Cl/ice.

of the CH<sub>3</sub>O group in compound **7**. The other two minima correspond to the zones located in the vicinity of the N atom in the connecting chain and in ring A. It should be noted that the  $V_{(r)\min}$  values, in the in-plane lone pair regions of N, are in accordance with previous findings,<sup>24</sup>

and indicate that these heteroatoms are H-bond acceptors.

It was particularly noteworthy that compounds **6** and **7** displayed almost the same antifungal activity. This

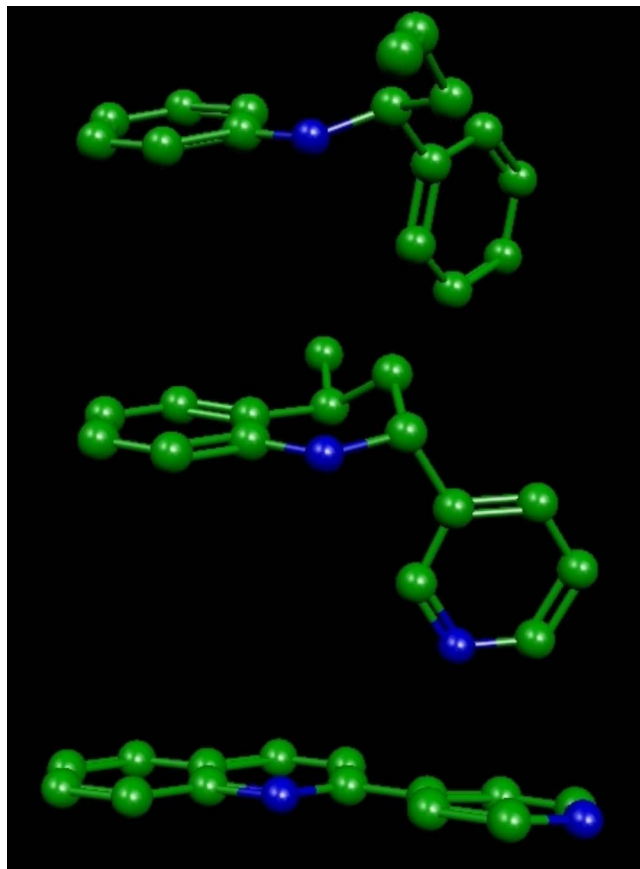


**Figure 1.** Spatial view of the preferred conformations obtained for homoallylamines, tetrahydroquinolines, and quinolines using RHF/6-31G(d) calculations.

result can be explained by the ability of compound **6** to adopt a conformation very similar to that of compound **7**. In this spatial ordering, the  $\text{CH}_3\text{O}$  group of ring B in compound **7** and the  $\text{CH}_3\text{O}$  group of ring A in compound **6** overlap, whereas the benzene ring A of **7** eclipses the benzene ring B of **6**. The similarity between the spatial ordering adopted by both compounds **6** and **7** is shown in Figure 3 where it is also possible to appreciate the similar spatial position for the lone pairs of their respective N atoms. In short, ring A of **7** is acting similarly to ring B in the whole structure of compound **6**. The antifungal activity shown by **6**, **7**, and **8** provides additional support for this hypothesis: whereas compounds **6** and **7** were active, compound **8** was inactive. It should be noted that the only structural difference between compounds **6** and **8** is the spatial position of the  $\text{OCH}_3$  group in ring A (in fact, they are simple positional isomers). It appears that the spatial orientation of the substituents in the general structural scaffold confers high affinity to the ligands. These results suggest that a spatially oriented molecular interaction (i.e., type hydrogen bond or dipole–dipole) could be operative in this case. Additional evidence for this hypothesis comes from the different activities of compounds **16**, **17**, and **18** as well as those displayed by **26**, **27**, and **28**. Note the different antifungal activity of these compounds as a function of the different positions of the nitrogen atom at ring B.

Based on these results we postulate a short-range electrostatic interaction for ring B, which may result in Brønsted (H-bonded) complex formation. Thus, in an exploratory theoretical study, we simulate the putative electrostatic interactions between the homoallylamine molecule and its molecular receptor in terms of representative smaller molecules. For instance, methyl alcohol was used to mimic the side chain of a serine residue which is a very good candidate to perform H-bonding interactions.<sup>25</sup> Alternative moieties present on ring B of homoallylamines were used as interacting counterparts (Scheme 2). The use of model compounds to calculate and simulate molecular interactions (MI) is necessary since homoallylamines are too large for accurate quantum mechanical MI calculations and the number of ligand models to be screened is large. We include electron correlation as well as solvation energies for studying the relative binding free energies of ligand–receptor interactions, which were demonstrated to be necessary in this type of calculations.<sup>25,26</sup>

The energies of interaction (EI) were calculated by approximation neglecting the superimposition of error due to the difference between the total energies of the complex with the sum of the total energies of the components:

$$\text{EI} = E_{\text{Cx}} - (E_{\text{BC}} + E_{\text{AC}}),$$

where EI is the energy interaction,  $E_{\text{Cx}}$  is the complex energy,  $E_{\text{BC}}$  is the energy of proton-donor component (i.e., Brønsted acid), and  $E_{\text{AC}}$  is the energy of proton acceptor component (i.e., Brønsted base).

The energies of all the complexes obtained and their components are summarized in Table 3. The interaction energies obtained for the different complexes are also shown in this table.

Figure 4 gives the different geometries obtained for complexes I–IV. The starting geometries of complexes I–III converged to the same kind of hydrogen-bonding interactions for such complexes, independent of the level of theory used. In contrast, complex IV displayed a clear electrostatic interaction but not hydrogen bonding because of an improper orientation.

Results obtained for complexes I–IV (Fig. 4 and Table 3) indicate that the most favored interaction occurs when the N atom of pyridine ring is acting as an acceptor, while the  $\text{CH}_3\text{–OH}$  group is the donor counterpart (compare the energies obtained for complexes I–IV, Table 3). These results are in agreement with our experimental data, showing that compounds possessing N and O groups at ring B are more active in comparison to those molecules possessing a S group.

Previous theoretical and crystallographic studies comparing oxygen and sulfur as H-bond acceptors showed that oxygen donates its  $n_{\sigma}$  lone pair, whereas sulfur donates its  $n_{\pi}$  lone pair.<sup>27,28</sup> Our results are in agreement with these results.





Scheme 2.

**2.2.2. Role of the connecting chain.** The lengthening of the flexible connecting chain caused a dramatic decrease in the antifungal activity. Compound **2**, which is the higher homologue of **3**, was inactive. In addition, compounds **32** and **33**, possessing an extra methylene group in the other side of the connecting chain, were also inactive compounds. It should be noted that **32** is a higher homologue of compound **15**. These results suggest that the distance between both aromatic rings A and B plays a critical role for the antifungal activity.

In order to obtain more information about the role of the allyl radical, we change the structure of the connecting-chain moiety. Elimination of the allyl moiety resulted in a slight increase of antifungal activity (compare compounds **7** and **14**). A comparative conformational study of these compounds was carried out from *ab initio* RH/3-21G calculations. The potential energy surfaces (PES) varying the torsional angles  $TA_1$  versus  $TA_2$  each  $30^\circ$  are shown in Figure 5. From this figure it is clear that the molecular flexibility of compound **14** is significantly higher than that obtained for compound **7** (note the different sizes of the dark zones in the contour diagrams and the different deeps and slopes of the valleys in the landscape diagrams). It appears that a more flexible connecting chain could facilitate the binding process.

**2.2.3. Role of ring A.** It appears that the presence of a non-substituted phenyl ring A leads to antifungal compounds (compounds **3**, **7**, **15**, and **25**). However, it should be noted that the presence of different substituents like  $CH_3$  or halogen as  $R_1$  enhances the antifungal activity (compare **17**, **19**, **20**, and **21** with **15**, and **27**, **29**, **30**, and **31** with **25**).

According to these results, ring A seems to play a central role in the recognition process. It was worthwhile to investigate how the change in distribution of charge due to the presence of  $CH_3$  or halogen substituents as  $R_1$  influences its nature. The knowledge of the inherent electronic properties of the ring A moiety of homoallylamines is important for rationalizing their complementarity with the binding site. To explore the degree of electronic changes in ring A due to the presence of halogen substituents at the  $R_1$  positions, MEPs of compounds **15**, **17**, and **21** were examined.

Electron density surfaces encoded with the electrostatic potential obtained by *ab initio* computations demonstrate that **17** and **21** have a closely related polarized electron distribution at ring A (Figs. 6b and c). In comparison, the analogous graph for compound **15** shows a very different and much less polarized electrostatic potential surface in this ring (Fig. 6a). On the basis of this

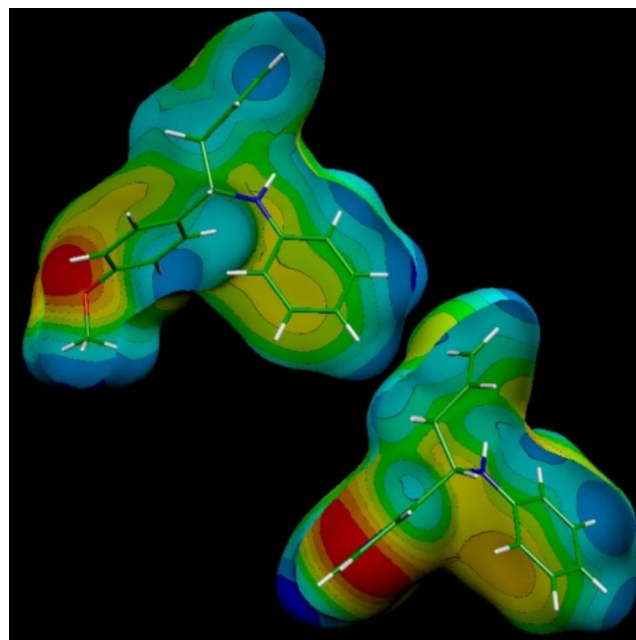


**Figure 2.** Electrostatic potential-encoded electron density surfaces of the core structures of compounds **7** and **15**. The surfaces were generated with Gaussian 03 after *ab initio* minimization with a 6-31G(d,p) basis set. The coloring represents electrostatic potential with red indicating the strongest attraction to a positive point charge and blue indicating the strongest repulsion. The electrostatic potential is the energy of interaction of the positive point charge with the nuclei and electrons of a molecule. It provides a representative measure of overall molecular charge distribution.

analysis, it becomes clear that replacing hydrogen with a bromide (or another halogen group) leads to a considerable perturbation of the electron distribution of ring A in these compounds. This electrostatic effect could offer a complementary surface in the binding pocket. The core structure of compound **21** could therefore represent the necessary electronic configuration to achieve significant antifungal activity.

At this stage of our SAR study, some general trends might be established. Compounds possessing both a halogen substituent (F, Cl or Br) at ring A and a heterocycle as ring B (pyridine, thiophene or furan) were the most active compounds in this series. Particularly noteworthy was the lack of activity obtained for compounds **9–11**, even though they possess halogen substituents at ring A. However, it should be noted that these homoallylamines have a non-substituted phenyl group as ring B. Thus, the lack of activity of these compounds highlights the importance of apparently two active centers for these compounds. Consequently, the antifungal activity of homoallylamines and their analogues reported here appears to be dependent on the combination of at least, two binding sites, one of them (ring B) possessing electronic characteristics to produce hydrogen bonds or polar interactions.

Finally we wish to discuss some details about a putative overall recognition process between the homoallylamine molecule and its potential biological receptor. On the

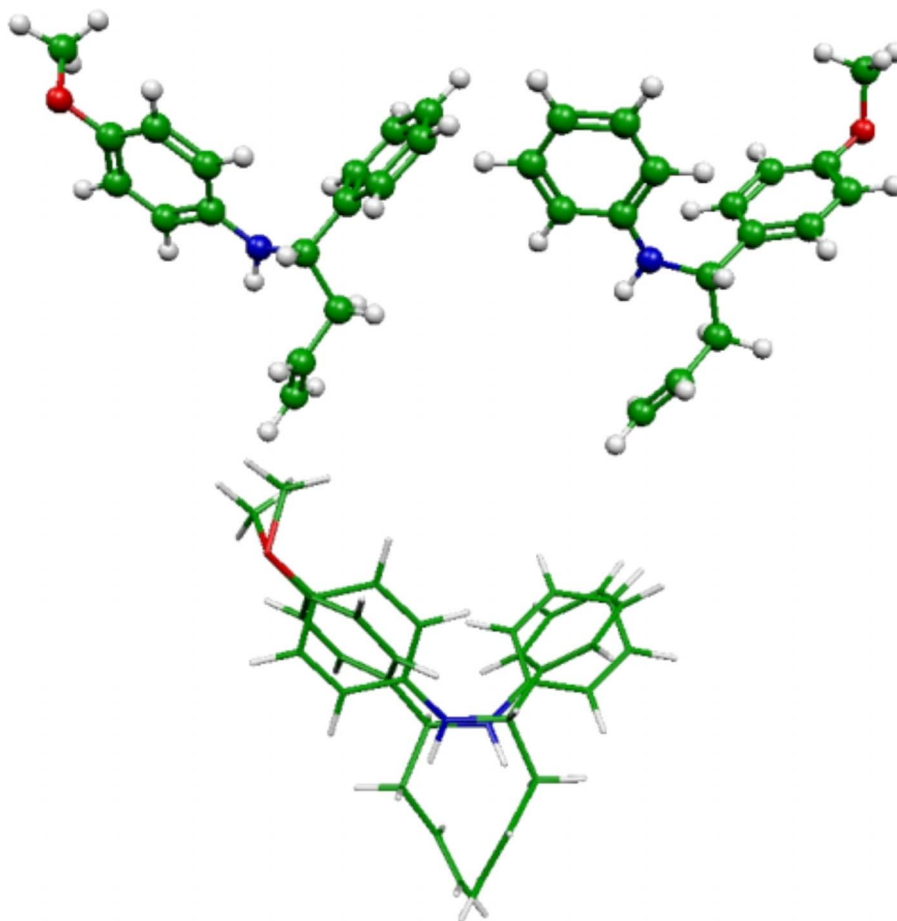


**Figure 3.** Stereo-view showing the superimposition of compounds **6** and **7** using the pharmacophoric sites ( $\text{CH}_3\text{O}$  group).

**Table 3.** Energies obtained at different levels of theory for the complexes and their components

	Complex energy (in hartrees)			Energy interaction of complexes (in $\text{kcal mol}^{-1}$ )		
	RHF/6-31G	RB3LYP/6-31++G**		RHF/6-31G	RB3LYP/6-31++G**	
		In vacuo	IPCM		In vacuo	IPCM
<b>I</b> —(methanol/3-methyl-pyridine)	−400,615862	−403,364558	−403,377316	−7.43	−4.61	−3.01
<b>II</b> —(methanol/1-methoxy-4-methyl-benzene)	−498,470371	−501,855868	−501,863450	−6.84	−4.27	−1.13
<b>III</b> —(methanol/2-methyl-furan)	−382,550885	−385,101265	−385,109571	−6.54	−3.96	−1.45
<b>IV</b> —(methanol/2-methyl-thiophene)	−705,208540	−708,072265	−708,080023	−3.18	−1.53	0.90
Energy of interacting components (in hartrees)						
3-Methyl-pyridine	−285,615852	−287,623346	−287,630355			
1-Methoxy-4-methyl-benzene	−383,471302	−386,115199	−386,119499			
2-Methyl-furan	−267,552296	−269,361090	−269,365107			
2-Methyl-thiophene	−590,215311	−592,335970	−592,339296			
Methanol	−114,988166	−115,733858	−115,742157			

Interaction energies obtained for the four complexes are also shown in this table.

basis of our results and using the simple notion of receptor-site occupancy, one may seek common chemical features between homoallylamines and their structurally related compounds to suggest chemical binding sites. Thus, we propose that the  $\text{OCH}_3$  group or the lone pairs of heteroatoms N, O or S atoms of ring B engage the receptor at a specific site (site I, Fig. 7). If homoallylamine engages the receptor at the site I, then it is possible to envisage that the rest of the homoallylamine

molecules contribute to the additional binding by interacting with at least one accessory region. The molecular structure of each of these compounds appears to be critical for antifungal activity. The fact that the activity is markedly affected by altering the length of the connecting chain suggests a co-operative effect between active groups, and one may consider that the second aromatic ring A makes a specific contribution to the binding via an aromatic ring orientation (site II, Fig. 7). In fact,



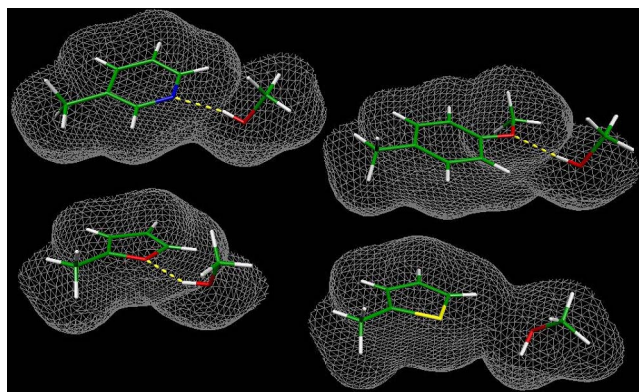


**Figure 4.** Spatial view of complexes I–IV obtained from RB3LYP/6-31++G(d,p) calculations. The interactions are shown as involving surface mesh.

there are various ways in which this moiety of the molecules may be involved. Thus, we may assume that a flat portion of the receptor could allow binding with the aromatic ring A of the antifungal compound through dispersion forces (van der Waals). An aromatic residue of the receptor could provide such a surface for example, but this is speculative. For the conformationally restricted compounds reported here, the proper “anchoring” of the benzene ring could be very important in a molecule to facilitate the binding mechanism. Thus, a kind of stepwise binding involving first site I followed by the rest of the molecule (site II) seems a reasonable possibility.

Since the molecules reported here are racemic, it is not possible to establish the potential role of the  $sp^3$  chiral carbon in the antifungal activity. It is clear that the resolution of the more active compounds into the two enantiomers could aid in establishing the difference between the activity of each one. A next step in our research will be the enantioselective syntheses of the most interesting molecules of the series.

### 3. Conclusions

We report here a new group of homoallylamine and tetrahydroquinoline derivatives acting as antifungal agents that adds information to previously reported studies.

Among them compounds **38** and **39** reported here and some of their congeners previously reported exhibited remarkable antifungal activity against dermatophyte fungi. A detailed SAR study supported by theoretical calculations helped us to identify and understand the minimal structural requirements for the antifungal action of these compounds.

On the basis of computational studies, it is possible to depict the salient structural requirements of homoallyl- amines and tetrahydroquinolines for displaying anti- fungal activity:

- Presence of two aromatic rings (rings A and B).
- Presence of a heteroatom (with electronic lone pairs) or  $CH_3O$  groups on ring B.
- A particular length of the connecting chain.
- Presence of a halogen atom (particularly Br or Cl) as  $R_1$  on ring A.

We believe our results may be helpful in the structural identification and understanding of the minimum structural requirements for these molecules and can provide a guide in the design of compounds with these inhibitory properties.

## 4. Experimental section

### 4.1. Chemistry

Melting points were determined with a Fisher–Johns melting point apparatus and are not corrected. Infrared spectra were recorded using KBr pellets on a Nicolet Avatar Model 360 FTIR spectrophotometer. Nuclear magnetic resonance spectra were measured on a Bruker AM 400 instrument (400 MHz  $^1H$  NMR and 100 MHz  $^{13}C$  NMR), using chloroform- $d$  as solvent and tetramethylsilane as internal standard. Chemical shifts ( $\delta$ ) and coupling constants ( $J$ ) are reported in ppm and Hz, respectively. A Hewlett–Packard (HP) 5890 A series II Gas Chromatograph interfaced to a HP 5972 Mass Selective Detector with a HP MS ChemStation Data system was used for MS identification. Elemental analyses were performed on a Perkin Elmer 2400 Series II analyzer and were within  $\pm 0.4$  of theoretical values.

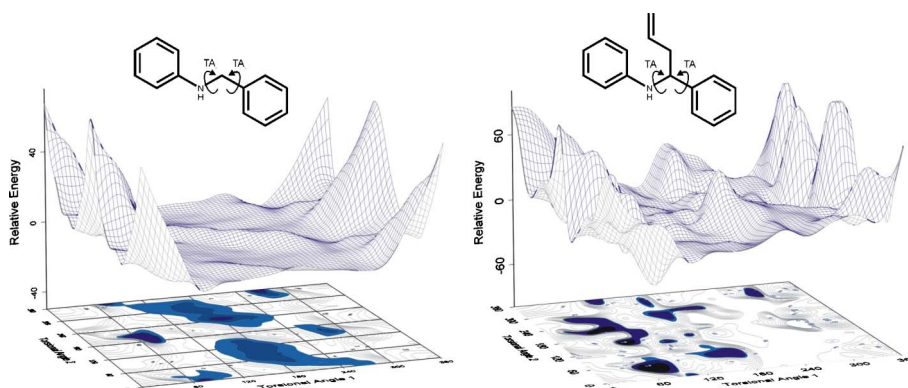


**Figure 5.** Relaxed conformational potential energy surfaces (PES),  $E = E(TA_1, TA_2)$  of compounds **7** and **14**. Top: energy landscape, bottom: energy contour representations.

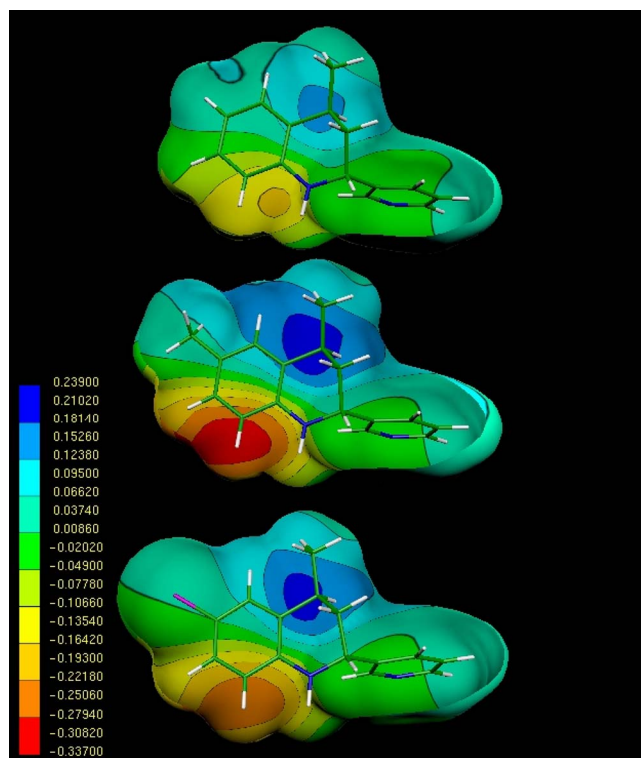


**Figure 6.** Electrostatic potential-encoded electron density surfaces of compounds **15** (a), **17** (b), and **21** (c). The surfaces were generated with Gaussian 03 after ab initio minimizations with a 6-31G(d,p) basis set. The color-coded is shown at the left.

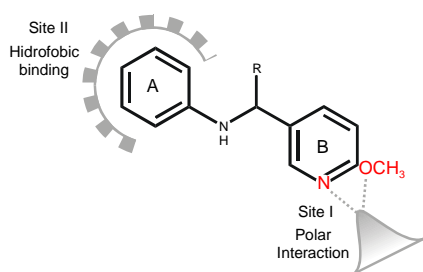


**Figure 7.** Schematic representation of a reduced model for the active sites of homoallylamine, showing the two putative binding sites (sites I and II).

The reaction progress was monitored using thin layer chromatography on a silufol UV<sub>254</sub> TLC aluminum sheet. Column chromatography (2 × 60 cm) was carried out using Merck silica gel 60 (230–400 mesh). All reagents and solvents were purchased from Merck, Sigma, and Aldrich Chemical Co., and were used without further purification.

Preparation of *N*-substituted anilines **12–14**, **32–38**, and **41–43** was realized according to reported methodologies.<sup>21,22</sup> Compounds **12** and **13** are known.<sup>29</sup>

**4.1.1. *N*-Benzyl-*N*-phenylamine (12).** Yellow oil. Yield 85%. IR (film):  $\nu$  3419, 1602 cm<sup>-1</sup> (s, NH). MS  $m/z$  (EI) 183 (M<sup>+</sup>, 61), 106 (19), 91 (100), 77 (23), 65 (25), 51 (16). Found: C, 85.45; H, 7.01; N, 7.44; calcd for C<sub>13</sub>H<sub>13</sub>N: C, 85.21; H, 7.15; N, 7.64.

**4.1.2. *N*-Benzyl-*N*-(4-ethylphenyl)amine (13).** Yellow oil. Yield 83%. IR (film):  $\nu$  3417, 1615 cm<sup>-1</sup> (s, NH). MS  $m/z$  (EI) 211 (M<sup>+</sup>, 63), 196 (70), 134 (11), 105 (4), 91 (100), 77 (10), 65 (14), 51 (4). Found: C, 85.10; H, 7.98; N, 6.91; calcd for C<sub>15</sub>H<sub>17</sub>N: C, 85.24; H, 7.66; N, 7.10.

**4.1.3. *N*-(4-Methoxybenzyl)-*N*-phenylamine (14).** Colorless crystals. Mp 61–62 °C. Yield 85%. IR (KBr):  $\nu$  3418, 1604 cm<sup>-1</sup> (s, NH). <sup>1</sup>H NMR:  $\delta$  7.31 (2H, d,  $J$  = 8.4 Hz, 3-H<sub>Bn</sub> and 5-H<sub>Bn</sub>), 7.19 (2H, t,  $J$  = 7.6 Hz, 3-H<sub>Ph</sub> and 5-H<sub>Ph</sub>), 6.89 (2H, d,  $J$  = 8.7 Hz, 2-H<sub>Bn</sub> and 6-H<sub>Bn</sub>), 6.75 (1H, t,  $J$  = 7.5 Hz, 4-H<sub>Ph</sub>), 6.67 (2H, d,  $J$  = 7.6 Hz, 2-H<sub>Ph</sub> and 6-H<sub>Ph</sub>), 4.27 (2H, s, -CH<sub>2</sub>-N), 3.82 (3H, s, CH<sub>3</sub>O); <sup>13</sup>C NMR (CDCl<sub>3</sub>):  $\delta$  158.9, 147.8, 131.1, 129.3, 129.2, 128.9, 128.8, 117.8, 114.0, 113.9, 113.2, 113.1, 55.3, 48.0. MS  $m/z$  (EI) 213 (M<sup>+</sup>, 29), 121 (100), 91 (4), 65 (3), 51 (3). Found: C, 78.55; H, 7.20; N, 6.20; calcd for C<sub>14</sub>H<sub>15</sub>NO: C, 78.84; H, 7.09; N, 6.57.

**4.1.4. *N*-(2-Furylmethyl)-*N*-phenylamine (34).** Yellow liquid. Yield 99%. IR (film):  $\nu$  3411, 1504 cm<sup>-1</sup> (s, NH). <sup>1</sup>H NMR:  $\delta$  7.40 (1H, dd,  $J$  = 2.0, 1.0 Hz, 5-H<sub>Fu</sub>), 7.22 (2H, m, 3-H<sub>Ph</sub> and 5-H<sub>Ph</sub>), 6.78 (1H, tt,  $J$  = 7.5, 1.0 Hz, 4-H<sub>Ph</sub>), 6.71 (2H, m, 2-H<sub>Ph</sub> and 6-H<sub>Ph</sub>), 6.35 (1H, dd,  $J$  = 3.0, 2.0 Hz, 4-H<sub>Fu</sub>), 6.27 (1H, dd,  $J$  = 3.0, 1.0 Hz, 3-H<sub>Fu</sub>), 4.34 (2H, s, -CH<sub>2</sub>-N), 4.04 (1H, br s, NH); <sup>13</sup>C NMR:  $\delta$  152.7, 147.6, 141.9, 129.2, 118.0, 113.1, 110.3, 106.9, 41.4. MS  $m/z$  (EI) 173 (M<sup>+</sup>, 39), 172 (25), 144 (6), 81 (100), 65 (10), 53 (33). Found: C, 76.56; H, 6.33; N, 8.20; calcd for C<sub>11</sub>H<sub>11</sub>NO: C, 76.28; H, 6.40; N, 8.09.

**4.1.5. *N*-(5-Methyl-2-furyl)methyl-*N*-phenylamine (35).** Yellow liquid. Yield 90%. IR (film):  $\nu$  3411, 1567 cm<sup>-1</sup> (s, NH); <sup>1</sup>H NMR:  $\delta$  7.22 (2H, m, 3-H<sub>Ph</sub> and 5-H<sub>Ph</sub>), 6.77 (1H, tt,  $J$  = 7.0, 1.0 Hz, 4-H<sub>Ph</sub>), 6.71 (2H, m, 2-H<sub>Ph</sub> and 6-H<sub>Ph</sub>), 6.14 (1H, d,  $J$  = 3.0 Hz, 4-H<sub>Fu</sub>), 5.93 (1H, dd,  $J$  = 3.0, 1.0 Hz, 3-H<sub>Fu</sub>), 4.28 (2H, s, -CH<sub>2</sub>-N), 3.95 (1H, br s, NH), 2.31 (3H, s, 5-CH<sub>3</sub>); <sup>13</sup>C NMR:  $\delta$  151.5, 150.7, 147.7, 129.1, 117.9, 107.8, 106.1, 41.5, 13.5. MS  $m/z$  (EI) 187 (M<sup>+</sup>, 19), 95 (100), 77 (10), 65 (9), 51 (10), 43 (16). Found: C, 76.55; H, 7.15; N, 7.20; calcd for C<sub>12</sub>H<sub>13</sub>NO: C, 76.98; H, 7.00; N, 7.48.

**4.1.6. *N*-(2-Furylmethyl)-*N*-(4-methoxyphenyl)amine (36).** Yellow solid. Mp 41 °C. Yield 95 %. IR (KBr):  $\nu$  3407 cm<sup>-1</sup> (s, NH). <sup>1</sup>H NMR:  $\delta$  7.35 (1H, dd,  $J$  = 2.0, 1.0 Hz, 5-H<sub>Fu</sub>), 6.80 (2H, m, 3-H<sub>Ph</sub> and 5-H<sub>Ph</sub>), 6.66 (2H, m, 2-H<sub>Ph</sub> and 6-H<sub>Ph</sub>), 6.33 (1H, dd,  $J$  = 3.0, 2.0 Hz, 4-H<sub>Fu</sub>), 6.23 (1H, dd,  $J$  = 3.5, 1.0 Hz, 3-H<sub>Fu</sub>), 4.28 (2H, s, -CH<sub>2</sub>-N), 3.63 (1H, br s, NH); <sup>13</sup>C NMR:  $\delta$  153.0, 152.5, 141.8, 114.8, 114.6, 110.3, 106.9, 55.7, 42.4. MS  $m/z$  (EI) 203 (M<sup>+</sup>, 64), 202 (34), 122 (86), 108 (6), 95 (15), 81 (100), 65 (8), 53 (41). Found: C, 71.05; H, 7.81; N, 6.33; calcd for C<sub>12</sub>H<sub>13</sub>NO<sub>2</sub>: C, 70.92; H, 6.45; N, 6.89.

**4.1.7. *N*-(4-Methoxyphenyl)-*N*-(5-methyl-2-furyl)methyl-amine (37).** Yellow liquid. Yield 98%. IR (film):  $\nu$  3411 cm<sup>-1</sup> (NH). <sup>1</sup>H NMR:  $\delta$  6.80 (2H, m, 3-H<sub>Ph</sub> and 5-H<sub>Ph</sub>), 6.67 (2H, m, 2-H<sub>Ph</sub> and 6-H<sub>Ph</sub>), 6.11 (1H, d,

$J = 3.0$  Hz, 4- $H_{Fu}$ ), 5.91 (1H, dd,  $J = 3.0, 1.0$  Hz, 3- $H_{Fu}$ ), 4.21 (2H, s,  $-CH_2-N$ ), 3.76 (3H, s, 4- $CH_3O$ ), 3.56 (1H, br s, NH);  $^{13}C$  NMR:  $\delta$  152.4, 151.4, 150.9, 141.9, 114.7, 107.7, 106.0, 55.6, 42.4, 13.45. MS  $m/z$  (EI) 217 ( $M^+$ , 17), 123 (24), 108 (10), 95 (100), 77 (3), 65 (4), 51 (4), 43 (11). Found: C, 71.55; H, 7.05; N, 6.20; calcd for  $C_{13}H_{15}NO_2$ : C, 71.87; H, 6.96; N, 6.45.

#### 4.1.8. *N*-(4-Bromophenyl)-*N*-(2-furylmethyl)amine (38).

Yellow solid. Mp 38 °C. Yield 97%. IR (KBr):  $\nu$  3415  $cm^{-1}$  (s, NH).  $^1H$  NMR:  $\delta$  7.40 (1H, dd,  $J = 2.0, 1.0$  Hz, 5- $H_{Fu}$ ), 7.29 (2H, m, 3- $H_{Ph}$  and 5- $H_{Ph}$ ), 6.57 (2H, m, 2- $H_{Ph}$  and 6- $H_{Ph}$ ), 6.36 (1H, dd,  $J = 3.0, 2.0$  Hz, 4- $H_{Fu}$ ), 6.26 (1H, dd,  $J = 3.0, 1.0$  Hz, 3- $H_{Fu}$ ), 4.30 (2H, s,  $-CH_2-N$ ), 4.10 (1H, br s, NH);  $^{13}C$  NMR:  $\delta$  152.1, 146.5, 142.0, 131.8, 114.6, 110.3, 109.5, 107.1, 41.2. MS  $m/z$  (EI) 252 ( $M^+$ , Br, 15), 251 (18), 91 (7), 81 (100), 63 (8), 53 (27). Found: C, 52.84; H, 4.20; N, 5.71; calcd for  $C_{11}H_{10}BrNO$ : C, 52.41; H, 4.00; N, 5.56.

#### 4.1.9. *N*-(4-Chlorophenyl)-*N*-(2-furylmethyl)amine (39).

Yellow liquid. Yield 99%. IR (film):  $\nu$  3415  $cm^{-1}$  (s, NH).  $^1H$  NMR:  $\delta$  7.38 (1H, dd,  $J = 2.0, 1.0$  Hz, 5- $H_{Fu}$ ), 7.14 (2H, m, 3- $H_{Ph}$  and 5- $H_{Ph}$ ), 6.60 (2H, m, 2- $H_{Ph}$  and 6- $H_{Ph}$ ), 6.34 (1H, dd,  $J = 3.5, 1.5$  Hz, 4- $H_{Fu}$ ), 6.24 (1H, dd,  $J = 3.0, 1.0$  Hz, 3- $H_{Fu}$ ), 4.29 (2H, s,  $-CH_2-N$ ), 4.06 (1H, br s, NH);  $^{13}C$  NMR:  $\delta$  152.2, 146.1, 142.0, 129.0, 122.5, 114.2, 110.3, 107.2, 41.4. MS  $m/z$  (EI) 207 ( $M^+$ ,  $^{35}Cl$ , 23), 206 (14), 81 (100), 75 (5), 63 (3), 53 (17). Found: C, 63.87; H, 4.63; N, 7.03; calcd for  $C_{11}H_{10}ClNO$ : C, 63.62; H, 4.85; N, 6.75.

#### 4.1.10. *N*-(4-Fluorophenyl)-*N*-(2-furylmethyl)amine (40).

Yellow liquid. Yield 99%. IR (film):  $\nu$  3413  $cm^{-1}$  (s, NH).  $^1H$  NMR:  $\delta$  7.39 (1H, dd,  $J = 2.0, 1.0$  Hz, 5- $H_{Fu}$ ), 6.91 (2H, m), 6.63 (2H, m, 3- $H_{Ph}$  and 5- $H_{Ph}$ ), 6.34 (1H, dd,  $J = 3.0, 2.0$  Hz, 2- $H_{Ph}$  and 6- $H_{Ph}$ ), 6.24 (1H, dd,  $J = 3.5, 1.0$  Hz, 4- $H_{Fu}$ ), 4.29 (2H, s,  $-CH_2-N$ ), 3.92 (1H, br s, NH);  $^{13}C$  NMR:  $\delta$  157.3, 154.9, 152.5, 143.9, 141.9, 115.7, 115.5, 114.1, 110.3, 107.0, 42.0. MS  $m/z$  (EI) 191 ( $M^+$ , 30), 190 (19), 95 (8), 81 (100), 75 (5), 53 (20). Found: C, 69.35; H, 5.43; N, 7.54; calcd for  $C_{11}H_{10}FNO$ : C, 69.10; H, 5.27; N, 7.33.

**4.1.11. *N*-(Thien-2-ylmethyl)aniline (41).** Yellow oil. Yield 95%. IR (film):  $\nu$  3411  $cm^{-1}$  (s, NH).  $^1H$  NMR:  $\delta$  7.23 (2H, t,  $J = 8.0, 3-H_{Ph}$  and 5- $H_{Ph}$ ), 7.19 (1H, dd,  $J = 4.0, 1.0, 5-H_{Thie}$ ), 6.96 (1H, dd,  $J = 4.0, 1.0, 3-H_{Thie}$ ), 6.95 (1H, t,  $J = 4.0, 4-H_{Thie}$ ), 6.82 (2H, d,  $J = 8.0, 2-H_{Ph}$  and 6- $H_{Ph}$ ), 6.75 (1H, d,  $J = 8.0, 4-H_{Ph}$ ), 4.68 (2H, s,  $-CH_2-N$ );  $^{13}C$  NMR:  $\delta$  148.4, 142.7, 126.7, 124.6, 124.2, 116.5, 129.1 (2C), 113.1 (2C), 49.5. MS  $m/z$  (EI) 189 ( $M^+$ , 33), 97 (100), 91 (3), 77 (15), 65 (9), 53 (10), 45 (15). Found: C, 69.73; H, 5.45; N, 7.52; calcd for  $C_{11}H_{11}NS$ : C, 69.80; H, 5.86; N, 7.40.

#### 4.1.12. *N*-(4-Methylphenyl)-*N*-(thien-2-ylmethyl)amine (42).

Yellow oil. Yield 96%. IR (film):  $\nu$  3408  $cm^{-1}$  (s, NH).  $^1H$  NMR:  $\delta$  7.20 (1H, dd,  $J = 4.0, 1.0, 5-H_{Thie}$ ), 7.06 (2H, d,  $J = 8.0, 3-H_{Ph}$  and 5- $H_{Ph}$ ), 6.97 (1H, t,  $J = 4.0, 3-H_{Thie}$ ), 6.94 (1H, dd,  $J = 4.0, 1.0, 4-H_{Thie}$ ), 6.76 (2H, d,  $J = 8.0, 2-H_{Ph}$  and 6- $H_{Ph}$ ), 4.66 (2H, s,  $-CH_2-N$ ), 2.28 (3H, s, 4- $CH_3$ );  $^{13}C$  NMR:  $\delta$  148.43 (1C), 142.7, 128.1 (2C), 126.8,

124.9, 124.3, 117.1, 113.9 (2C), 49.5, 20.1. MS  $m/z$  (EI) 203 ( $M^+$ , 31), 97 (100), 91 (7), 77 (7), 65 (6), 53 (8), 45 (6). Found: C, 71.02; H, 6.67; N, 6.54; calcd for  $C_{12}H_{13}NS$ : C, 70.89; H, 6.45; N, 6.89.

#### 4.1.13. *N*-(3-Methylphenyl)-*N*-(thien-2-ylmethyl)amine (43).

Yellow oil. Yield 97%. IR (film):  $\nu$  3408  $cm^{-1}$  (s, NH).  $^1H$  NMR:  $\delta$  7.21 (1H, dd,  $J = 5.0, 1.0, 5-H_{Thie}$ ), 6.98 (1H, dd,  $J = 4.0, 3.0, 4-H_{Thie}$ ), 6.97 (1H, t,  $J = 7.5, 5-H_{Ph}$ ), 6.96 (1H, dd,  $J = 4.0, 2.0, 3-H_{Thie}$ ), 6.67 (1H, s, 2- $H_{Ph}$ ), 6.66 (1H, d,  $J = 7.0, 6-H_{Ph}$ ), 6.60 (1H, d,  $J = 7.0, 4-H_{Ph}$ ), 4.69 (2H, s,  $-CH_2-N$ ), 2.34 (3H, s, 3- $CH_3$ );  $^{13}C$  NMR:  $\delta$  148.6, 142.9, 138.8, 129.0, 126.7, 124.6, 124.2, 118.1, 113.8, 110.3, 49.4, 21.9. MS  $m/z$  (EI) 203 ( $M^+$ , 42), 97 (100), 91 (9), 77 (7), 65 (7), 53 (8), 45 (8). Found: C, 70.77; H, 6.76; N, 6.73; calcd for  $C_{12}H_{13}NS$ : C, 70.89; H, 6.45; N, 6.89.

Preparation of *N*-aryl-*N*-[1-(thien-2-yl)but-3-enyl]amines **44**, **45** was realized according to reported methodologies.<sup>16,17</sup>

#### 4.1.14. *N*-(1-thien-2-yl)but-3-enylaniline (44).

Yellow viscous oil. Bp 124–126 °C/1 mm Hg. Yield 70%. IR (film):  $\nu$  3405 (s, NH), 1639 (s,  $C=C$ ), 920  $cm^{-1}$  (s,  $=CH_2$ ).  $^1H$  NMR:  $\delta$  7.18 (1H, dd,  $J = 4.0, 1.0$  Hz, 5- $H_{Thie}$ ), 7.14 (2H, t,  $J = 8.0$  Hz, 3- $H_{Ph}$  and 5- $H_{Ph}$ ), 6.99 (1H, d,  $J = 4.0$  Hz, 4- $H_{Thie}$ ), 6.95 (1H, dd,  $J = 4.0, 1.0$  Hz, 3- $H_{Thie}$ ), 6.71 (1H, t,  $J = 8.0$  Hz, 4- $H_{Ph}$ ), 6.61 (2H, d,  $J = 8.0$  Hz, 2- $H_{Ph}$  and 6- $H_{Ph}$ ), 5.82 (1H, m,  $-CH=$ ), 5.19 (2H, m,  $=CH_2$ ), 4.72 (1H, t,  $J = 8.0$  Hz, 1-H), 2.67 (2H, m,  $-CH_2-$ );  $^{13}C$  NMR:  $\delta$  148.6, 147.0, 134.0, 129.1, 126.8, 123.7, 123.4, 118.0, 113.6, 53.4, 43.1. MS  $m/z$  (EI) 229 ( $M^+$ , 4), 188 (100), 104 (21), 97 (5), 91 (4), 83 (1), 77 (25), 63 (2). Found: C, 73.55; H, 6.34; N, 6.20; calcd for  $C_{14}H_{15}NS$ : C, 73.32; H, 6.59; N, 6.11.

#### 4.1.15. *N*-(4-Methylphenyl)-*N*-(1-thien-2-yl)but-3-enylaniline (45).

Yellow viscous oil. Bp 120–122 °C/1 mm Hg. Yield 77%. IR (film):  $\nu$  3403 (s, NH), 1639 (s,  $C=C$ ), 919  $cm^{-1}$  (s,  $=CH_2$ ).  $^1H$  NMR:  $\delta$  7.17 (1H, dd,  $J = 4.0, 1.0$  Hz, 5- $H_{Thie}$ ), 6.99 (1H, dd,  $J = 4.0, 1.0$  Hz, 4- $H_{Thie}$ ), 6.97 (1H, t,  $J = 4.0$  Hz, 3- $H_{Thie}$ ), 6.96 (2H, d,  $J = 8.0$  Hz, 3- $H_{Ph}$  and 5- $H_{Ph}$ ), 6.55 (2H, d,  $J = 8.0$  Hz, 2- $H_{Ph}$  and 6- $H_{Ph}$ ), 5.81 (1H, m,  $-CH=$ ), 5.19 (2H, m,  $=CH_2$ ), 4.69 (1H, t,  $J = 8.0$  Hz, 1-H), 2.67 (2H, m,  $-CH_2-$ ), 2.23 (3H, s, 4- $CH_3$ );  $^{13}C$  NMR:  $\delta$  148.9, 144.7, 129.6, 134.2, 127.2, 126.7, 123.7, 123.4, 118.51, 113.8, 53.8, 43.1, 20.4. MS  $m/z$  (EI) 243 ( $M^+$ , 5), 202 (100), 186 (2), 118 (13), 111 (1), 105 (2), 97 (5), 91 (20), 77 (5). Found: C, 73.87; H, 7.22; N, 5.63; calcd for  $C_{15}H_{17}NS$ : C, 74.03; H, 7.04; N, 5.76.

**4.1.16. Microorganisms and media.** For the antifungal evaluation, strains from the American Type Culture Collection (ATCC), Rockville, MD, USA, and CERE-MIC (C), Centro de Referencia Micológica, Facultad de Ciencias Bioquímicas y Farmacéuticas, Suipacha 531-(2000)-Rosario, Argentina, were used: *Microsporum canis* C 112, *Microsporum gypseum* C 115, *Trichophyton rubrum* C 110, *Trichophyton mentagrophytes* ATCC 9972, and *Epidermophyton floccosum* C 114. Strains were



grown on Sabouraud-chloramphenicol agar slants for 48 h at 30 °C, maintained on slopes of Sabouraud-dextrose agar (SDA, Oxoid), and subcultured every 15 days to prevent pleomorphic transformations. Inocula of spore suspensions were obtained according to reported procedures<sup>30</sup> and adjusted to  $1-5 \times 10^3$  spores with colony-forming units (CFU)/ml.

**4.1.17. Antifungal susceptibility testing.** The minimal inhibitory concentration (MIC) of each extract was determined by using broth microdilution techniques following the guidelines of the National Committee for Clinical Laboratory Standards for filamentous fungi (M-38A) (NCCLS, 2002).<sup>31</sup> MIC values were determined in RPMI-1640 (Sigma, St. Louis, MO, USA) buffered to a pH 7.0 with MOPS. Microtiter trays were incubated at 35 °C for yeasts and hialophyphomycetes, and at 28–30 °C for dermatophyte strains in a moist, dark chamber, and MICs were recorded at 48 h for yeasts, and at a time according to the control fungus growth, for the rest of fungi. The susceptibilities of the standard drugs Ketoconazole, Terbinafine, and Amphotericin B were defined as the lowest concentration of drug which resulted in total inhibition of fungal growth.

For the assay, extract stock solutions were twofold diluted with RPMI-1640 from 250 to 0.98 µg/ml (final volume = 100 µl) and a final DMSO concentration ≤1%. A volume of 100 µl of inoculum suspension was added to each well with the exception of the sterility control where sterile water was added to the well instead. The MIC was defined as the minimum inhibitory concentration of the extract which resulted in total inhibition of the fungal growth.

**4.1.18. Computational methods.** All calculations were carried out using the Gaussian 03 program.<sup>32</sup> The search for low-energy conformations on the potential energy surface for homoallylamines reported here was carried out by first using the systematic routine GASCOS<sup>33–36</sup> in connection with the MM2 force field. Subsequently, ab initio (RHF/6-31G(d)) calculations were used in the geometry optimization jobs. Minima were characterized through harmonic frequency analysis.

For the molecular interaction (MI) simulations, all the complexes under investigation were initially optimized using the RHF/6-31G(d) level of theory. Correlation effects were included using the density functional theory (DFT) with the Becke-3-Lee–Yang–parr (RB3LYP)<sup>37</sup> functional and 6-31++G(d,p) basis set for all the complexes obtained at the lower level of computation. During the DFT calculations, the RHF/6-31G geometries were kept fixed.

The conformational potential energy surfaces (PESs) reported here for compounds **7** and **14**, with 169 grid points, were generated using 30° steps along both dimensions (TA1 and TA2).

The electronic study of the compounds was carried out by using molecular electrostatic potentials (MEPs). MEPs have been shown to provide reliable information,

both on the interaction sites of the molecules with point charges and on the comparative reactivities of these sites.<sup>38–41</sup> These MEPs were calculated from RHF/6-31G(d,p) wave functions using the SPARTAN program.<sup>42</sup> All the calculations were performed on a cluster of PC Pentium 4. Each MI optimizations takes about 48 h. Previous reports<sup>25,26</sup> indicate that it is necessary to include correlation energy corrections and solvent effects in these calculations to obtain reliable results.

### Acknowledgments

This work was supported by grants from Universidad Nacional de San Luis and Agencia de Promoción Científica y Tecnológica de la Argentina (PICTR #00260). This work is part of the Iberoamerican Project PIBEA-FUN X.7 (Search and development of new antifungal agents) of CYTED (Iberoamerican Program of Science and Technology for the Development) Subprogram X. R. D. Enriz is a member of the CONICET (Argentina) staff. V.K. thanks Instituto Colombiano para el Desarrollo de la Ciencia y la Tecnología 'Francisco José de Caldas' (COLCIENCIAS, Proyecto: 1102-05-11429) for financial support and Dr. Arilio R. Palma for providing some thiophene derivatives.

### References and notes

1. Zacchino, S.; Yunes, R.; Cechinel Filho, V.; Enriz, D.; Kouznetsov, V.; Ribas, J. C. In *Plant-Derived Antimycotics Current Trends and Future Prospects*; Rai, M., Mares, D., Eds.; Haworth Press: New York, 2003; pp 1–47.
2. Ablordeppey, S.; Fan, P.; Ablordeppey, J.; Mardenborough, L. *Curr. Med. Chem.* **1999**, *6*, 1151.
3. Li, D.; Calderone, R. In *Pathogenic Fungi, Host Interaction and Emerging Strategies for Control*; San-Blas, G., Calderone, R., Eds.; Caister Academic Press: Norfolk, 2004; pp 335–355.
4. Marr, K.; Borden, R. *Clin. Microbiol. Rev.* **1998**, *11*, 382.
5. San Blas, G. *Revista Iberoamer. Micol.* **1991**, *8*, 28.
6. Onishi, J.; Meinz, M.; Curotto, J.; Dreikorn, S.; Rosenbach, M.; Douglas, C.; Abruzzo, G.; Flattery, A.; Kong, L.; Cabello, A.; Vicente, F.; Pelaez, F.; Diez, M.; Martin, I.; Bills, G.; Giacobbe, R.; Dombrowski, A.; Schwartz, R.; Morris, S.; Harris, G.; Tsipouras, A.; Wilson, K.; Kurtz, M. *Antimicrob. Agents Chemother.* **2000**, *44*, 368.
7. Selitrennikoff, C. *Antifungal Drugs: (1,3)β-Glucan-Synthase Inhibitors*; Springer-Verlag: Heidelberg, 1995, pp 1–12.
8. Pérez, P.; Ribas, J. C. *Methods* **2004**, *33*, 245.
9. Zacchino, S.; Rodriguez, G.; Pezzenati, G.; Orellana, G.; Enriz, R. D.; Gonzalez Sierra, G. *J. Nat. Prod.* **1997**, *60*, 661.
10. Zacchino, S.; Rodríguez, G.; Santecchia, C.; Pezzenati, G.; Giannini, F.; Enriz, R. D. *J. Ethnopharmacol.* **1998**, *62*, 35.
11. Zacchino, S.; Lopez, S.; Pezzenati, G.; Furlan, R.; Santecchia, C.; Muñoz, L.; Giannini, F.; Rodríguez, A. M.; Enriz, R. D. *J. Nat. Prod.* **1999**, *63*, 1353.
12. Freile, M. L.; Giannini, F.; Pucci, G.; Sturniolo, A.; Rodero, L.; Pucci, O.; Balzaretta, V.; Enriz, R. D. *Fitoterapia* **2003**, *74*, 702.
13. Lopez, S. N.; Castelli, M. V.; Zacchino, S.; Dominguez, J.; Lobo, G.; Charris-Charris, J.; Cortez, J.; Ribas, J.; Devia, C.; Rodriguez, A. M.; Enriz, R. D. *Bioorg. Med. Chem.* **2001**, *9*, 1999.

14. Karolyhazy, K.; Freile, M. L.; Anwair, M.; Beke, Gy.; Giannini, F.; Sortino, M.; Ribas, J. C.; Zacchino, S.; Matyus, P.; Enriz, R. D. *Arzneim.-Forsch.-Drug Res.* **2003**, *53*, 738.
15. Giannini, F. A.; Aimar, M. L.; Sortino, M. A.; Gomez, R.; Sturniolo, A.; Juarez, A.; Zacchino, S.; de Rossi, R. H.; de Enriz, R. D. *Il Farmaco.* **2004**, *59*, 245.
16. Kouznetsov, V. V.; Urbina, J.; Palma, A.; López, S.; Ribas, J.; Enriz, R. D.; Zacchino, S. *Bioorg. Med. Chem.* **2000**, *8*, 691.
17. Vargas, L. Y.; Castelli, M.; Kouznetsov, V.; Urbina, J. M.; Lopez, S.; Sortino, M.; Enriz, R. D.; Ribas, J. C.; Zacchino, S. *Bioorg. Med. Chem.* **2003**, *11*, 1531.
18. Villagra, S. E.; Bernini, M. C.; Rodriguez, A. M.; Zacchino, S.; Kouznetsov, V.; Enriz, R. D. *J. Mol. Struct. (Theochem)* **2003**, *587*, 666–667.
19. Layer, R. W. *Chem. Rev.* **1963**, *63*, 489.
20. Ochoa Puentes, C.; Kouznetsov, V. J. *Heterocycl. Chem.* **2002**, *39*, 595.
21. Borch, R. F.; Bernstein, M. D.; Durst, H. D. *J. Am. Chem. Soc.* **1971**, *93*, 2897.
22. Stork, G.; Brizzolara, A.; Landesman, H.; Szmuszkowicz, J.; Terrell, R. J. *Am. Chem. Soc.* **1963**, *85*, 207.
23. Srebenik, S.; Weinstein, M.; Pauncz, R. *Chem. Phys. Lett.* **1973**, *20*, 419.
24. Craven, B. M.; Benci, P. *Acta Crystallogr.* **1981**, *337*, 1588.
25. Suvire, F. D.; Cabedo, N.; Chagraoui, A.; Zamora, M. A.; Cortes, D.; Enriz, R. D. *J. Mol. Struct. (Theochem)* **2003**, *455*, 666–667.
26. Suvire, F. D.; Rodriguez, A. M.; Mak, M. L.; Papp, J. Gy.; Enriz, R. D. *J. Mol. Struct. (Theochem)* **2003**, *540*, 271.
27. Platts, J. A.; Howard, S. T.; Bracke, B. R. F. *J. Am. Chem. Soc.* **1996**, *118*, 2726.
28. Salai Ceettu Ammal, S.; Venuvanalinam, P. J. *Chem. Soc. Faraday Trans.* **1998**, *94*, 2669.
29. Billman, J. H.; Diesing, A. C. *J. Org. Chem.* **1957**, *22*, 1068.
30. Wright, L.; Scott, E.; Gorman, S. J. *Antimicrob. Chemother.* **1983**, *12*, 317.
31. NCCLS, *National Committee for Clinical Laboratory Standards, Method M-38A*, 2nd ed.; Wayne, Eds.; 2002; Vol. 22 (16), pp 1–27.
32. Frisch, M. J.; Trucks, G. W.; Schlegel, H. B.; Scuseria, G. E.; Robb, M. A.; Cheeseman, J. R.; Montgomery, J. A., Jr.; Vreven, T.; Kudin, K. N.; Burant, J. C.; Millam, J. M.; Iyengar, S. S.; Tomasi, J.; Barone, V.; Mennucci, B.; Cossi, M.; Scalmani, G.; Rega, N.; Petersson, G. A.; Nakatsuji, H.; Hada, M.; Ehara, M.; Toyota, K.; Fukuda, R.; Hasegawa, J.; Ishida, M.; Nakajima, T.; Honda, Y.; Kitao, O.; Nakai, H.; Klene, M.; Li, X.; Knox, J. E.; Hratchian, H. P.; Cross, J. B.; Adamo, C.; Jaramillo, J.; Gomperts, R.; Stratmann, R. E.; Yazyev, O.; Austin, A. J.; Cammi, R.; Pomelli, C.; Ochterski, J. W.; Ayala, P. Y.; Morokuma, K.; Voth, G. A.; Salvador, P.; Dannenberg, J. J.; Zakrzewski, V. G.; Dapprich, S.; Daniels, A. D.; Strain, M. C.; Farkas, O.; Malick, D. K.; Rabuck, A. D.; Raghavachari, K.; Foresman, J. B.; Ortiz, J. V.; Cui, Q.; Baboul, A. G.; Clifford, S.; Cioslowski, J.; Stefanov, B. B.; Liu, G.; Liashenko, A.; Piskorz, P.; Komaromi, I.; Martin, R. L.; Fox, D. J.; Keith, T.; Al-Laham, M. A.; Peng, C. Y.; Nanayakkara, A.; Challacombe, M.; Gill, P. M. W.; Johnson, B.; Chen, W.; Wong, M. W.; Gonzalez, C.; Pople, J. A. *Gaussian 03, Revision B.05*, 2003, Gaussian, Inc., Pittsburgh, PA.
33. Santágata, L. N.; Suvire, F. D.; Enriz, R. D.; Torday, L. L.; Csizmadia, I. G. *J. Mol. Struct. (Theochem)* **1999**, *465*, 33.
34. Santágata, L. N.; Suvire, F. D.; Enriz, R. D. *J. Mol. Struct. (Theochem)* **2000**, *507*, 89.
35. Santágata, L. N.; Suvire, F. D.; Enriz, R. D. *J. Mol. Struct. (Theochem)* **2001**, *536*, 173.
36. Santágata, L. N.; Suvire, F. D.; Enriz, R. D. *J. Mol. Struct. (Theochem)* **2001**, *571*, 91.
37. (a) Becke, A. D. *Phys. Rev. A* **1998**, *38*, 3098–3100; (b) Becke, A. D. *J. Chem. Phys.* **1993**, *98*, 5618–5652; (c) Lee, C.; Yang, W.; Parr, R. G. *Phys. Rev. B* **1998**, *37*, 785–789.
38. Politzer, P.; Truhlar, D. G. *Chemical Applications of Atomic and Molecular Electrostatic Potentials*; Plenum Publishing: New York, 1991.
39. Carrupt, P. A.; El Tayar, N.; Karlé, A.; Festa, B. *Methods Enzymol.* **1991**, *202*, 638.
40. Greeling, P.; Langenaeker, W.; De Proft, F.; Baeten, A.. In *Molecular Electrostatic Potentials: Concepts and Applications. Theoretical and Computational Chemistry*; Elsevier Science B.V.: Amsterdam, 1996; Vol. 3, pp 587–617.
41. Jáuregui, E. A.; Ciuffo, G. M.; Enriz, R. D. *Temas Actuales de Química Cuántica*; UAM Ediciones, 1997; Vol. 29, pp 327–349.
42. *PC SPARTAN PRO* Wavefunction, Inc., Pittsburg, PA (1996–2000).